Spectrochimica Acta Part A: Molecular and Biomolecular Spectroscopy 95 (2012) 658–663

Contents lists available at SciVerse ScienceDirect

Spectrochimica Acta Part A: Molecular and Biomolecular Spectroscopy

journal homepage: www.elsevier.com/locate/saa

A rhodamine chromene-based turn-on fluorescence probe for selectively imaging Cu^{2+} in living cell

Wei-Yong Liu [a,1], Hai-Ying Li [b,1], Hong-Shui Lv [a], Bao-Xiang Zhao [a,*], Jun-Ying Miao [b,*]

[a] Institute of Organic Chemistry, School of Chemistry and Chemical Engineering, Shandong University, Jinan 250100, PR China
[b] Institute of Developmental Biology, School of Life Science, Shandong University, Jinan 250100, PR China

HIGHLIGHTS

- A new fluorescence probe was synthesized to improve membrane-permeable property.
- The probe can monitor Cu^{2+} in living cells with high sensitivity and selectivity.
- The probe can monitor intracellular Cu^{2+} in HeLa cells in shorter time.

GRAPHICAL ABSTRACT

Rhodamine chromene-based "turn-on" fluorescence probe can monitor the intracellular Cu^{2+} level in living HeLa cells with high sensitivity and selectivity in shorter time.

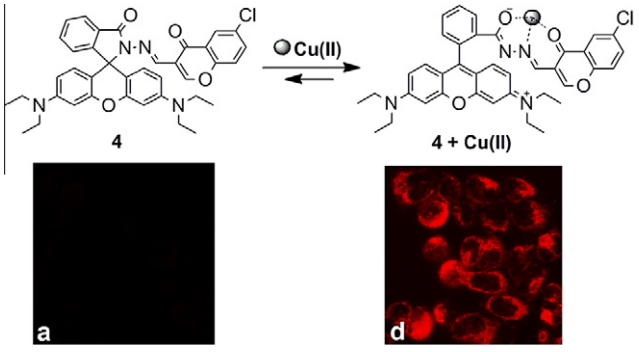

ARTICLE INFO

Article history:
Received 6 March 2012
Received in revised form 13 April 2012
Accepted 18 April 2012
Available online 26 April 2012

Keywords:
Rhodamine chromene
X-ray
Fluorescence probe
Copper ion
Living cells

ABSTRACT

We describe the development of a rhodamine chromene-based turn-on fluorescence probe to monitor the intracellular Cu^{2+} level in living cells. The new fluorescent probe with a chlorine group in chromene moiety exhibits good membrane-permeable property than previous reported because the predicted lipophilicity of present probe **4** is stronger than that of methoxyl substituted probe in our previous work (CLogP of **4**: 8.313, CLogP of methoxyl substituted probe: 7.706), and a fluorescence response toward Cu^{2+} under physiological conditions with high sensitivity and selectivity, and facilitates naked-eye detection of Cu^{2+}. The fluorescence intensity was remarkably increased upon the addition of Cu^{2+} within 1 or 2 min, while the other sixteen metal ions caused no significant effect.

Introduction

Copper, after zinc and iron, ranks third in abundance in human bodies among the essential heavy metals [1]. Copper plays a critical role in the physiology of living organisms and has multiple functions, as iron absorption, hemopoiesis, and diverse enzyme activities and in the redox processes. However, alteration in the cellular homeostasis of copper ions is connected to various severe neurodegenerative diseases such as Menkes syndrome, Wilson's disease, amyotrophic lateral sclerosis, and Alzheimer's disease

* Corresponding authors. Tel.: +86 531 88366425; fax: +86 531 88564464 (B.-X. Zhao).
E-mail addresses: bxzhao@sdu.edu.cn (B.-X. Zhao), miaojy@sdu.edu.cn (J.-Y. Miao).
[1] These two authors are equally contributed to this work.

1386-1425/$ - see front matter © 2012 Elsevier B.V. All rights reserved.
http://dx.doi.org/10.1016/j.saa.2012.04.073

[2]. Furthermore, a higher level of Cu^{2+} is detected in tumors with a possible role in promoting angiogenesis (new blood vessel growth) [3]. Moreover, with excessive loading, Cu^{2+} is highly toxic to organisms [4]. Therefore, the quantitative detection of intracellular Cu^{2+} is of great importance for elucidating its complex physiological and pathological roles.

The design and synthesis of chemosensors for copper ions has become a very highly focused area of research, as a result of the demand for more sensitive and selective chemosensors for imaging in living cells and in vivo purposes [5]. A number of fluorescent probes based on coumarin [6], 1,3,5-triphenylbenzene fluorophore [7], *N*-(quinolin-8-yl)acetamide [8], dansyl-anthracene dyads [9], nanoparticle [10], polymer-based [11] with high sensitivity and specificity toward Cu^{2+} have been developed.

It is known that the rhodamine framework is an ideal mode to construct fluorescent chemosensors, because the spirolactam ring-opening process leads to a turn-on fluorescence change with excellent photophysical properties, such as long absorption and emission wavelengths, large absorption coefficient, and high fluorescence quantum yield [12]. An additional advantage of such a rhodamine-based sensing system is that the ring-opening process is also accompanied by a vivid color change from colorless to pink, thus enabling the metal detection with the naked eye [13].

Although a number of rhodamine-based fluorescent probes for transition metals including zinc, iron, chromium and mercury have been developed over the past decades [14–17], relatively few copper-selective probes have been reported [5j,18]. Among these probes, membrane-permeable chemosensors that allow monitoring of intracellular copper are rare [5j,5k,18b,18d,18e]. Thus, the development of turn-on fluorescent probes with high sensitivity and selectivity for monitoring Cu^{2+} in living cells remains a significant challenge. Due to the good stability of Schiff base ligands with Cu^{2+} to form complexes [19], rhodamine Schiff base ligands based fluorescence probe have attracted a great deal of attention in recent years [14a,17e,18a,18g,20]. In our previous paper, we described a rhodamine chromene-based fluorescence probe to monitor the intracellular Cu^{2+} level in living cells [21]. Due to the less membrane permeation ability of the probe, the incubation of the probe needs 5 h to take fluorescence microscope images of living HeLa cells. Hence, in order to increase the membrane permeation ability of the probe, we modified the structure of the probe by introducing a chlorine atom to chromene moiety because the predicted lipophilicity of the probe with chlorine instead of methoxyl group is stronger. In addition, a smaller size of chlorine atom compared to methoxyl group was expected to improve the cell permeability of the probe. The results showed that the modified probe not only possess higher fluorescence intensity but also have favorable membrane permeation ability for the detection of the intracellular Cu^{2+} level in living cells.

Experimental

Materials and characterization

Deionized water was used throughout the experiment. All the reagents were purchased from commercial suppliers and used without further purification. The solutions of metal ions were prepared from $NaNO_3$, $Mg(NO_3)_2{\cdot}6H_2O$, $Al(NO_3)_3{\cdot}9H_2O$, KNO_3, $Ca(NO_3)_2{\cdot}4H_2O$, $Cr(NO_3)_3{\cdot}9H_2O$, 50% (wt.) $Mn(NO_3)_2$ (aq.), $Fe(NO_3)_3{\cdot}9H_2O$, $Co(NO_3)_2{\cdot}6H_2O$, $Ni(NO_3)_2{\cdot}6H_2O$, $Cu(NO_3)_2{\cdot}3H_2O$, $Zn(NO_3)_2{\cdot}6H_2O$, $AgNO_3$, $Cd(NO_3)_2{\cdot}4H_2O$, $Ba(NO_3)_2$, $Hg(NO_3)_2{\cdot}H_2O$, $Pb(NO_3)_2$, $CuCl_2{\cdot}2H_2O$, $CuSO_4{\cdot}5H_2O$, $Cu(Ac)_2{\cdot}H_2O$, NaCl, NaAc and Na_2SO_4, respectively, and were dissolved in distilled water. All samples were prepared at room temperature, shaken for 10 s and stood for 18 h before UV–vis and fluorescence determination. Thin-layer chromatography (TLC) was conducted on silica gel 60 F254 plates (Merck KGaA). HEPES buffer solutions (pH 7.2) were prepared using 20 mM HEPES, and the appropriate amount of aqueous sodium hydroxide using a pH meter. ^{1}H NMR (400 MHz) and ^{13}C NMR (100 MHz) spectra were recorded on a Bruker Avance 400 spectrometer using $CDCl_3$ as solvent and tetramethylsilane (TMS) as internal standard. Melting points were determined on an XD-4 digital micro melting point apparatus. IR spectra were recorded with an IR spectrophotometer VERTEX 70 FT-IR (Bruker Optics). HRMS spectra were recorded on a Q-TOF6510 spectrograph (Agilent). UV–vis spectra were recorded on a U-4100 (Hitachi). Fluorescent measurements were recorded on a Perkin Elmer LS-55 luminescence spectrophotometer.

Cell culture and imaging

HeLa cells were cultured in a Dulbecco's modified Eagle's medium (DMEM, Gibco) containing 10% calf bovine serum (HyClone) at 37 °C in humidified air and 5% CO_2. For fluorescence imaging, the cells (5×10^4 mL^{-1}) were seeded into 24-well plates, and experiments to assay Cu^{2+} uptake were performed in the same media supplemented with 50 μM of $CuCl_2$ or $Cu(NO_3)_2$ for 2 h. The cells were washed twice with PBS buffer before the staining experiments, and incubated with 10 μM of probe **4** for 1 h in the incubator. After washing twice with PBS, the cells were imaged under a Phase Contrast Microscope (Nikon, Japan).

(E)-2-((6-Chloro-4-oxo-4H-chromen-3-yl)methyleneamino)-3′,6′-bis(diethylamino)spiro[isoindoline-1,9′-xanthen]-3-one (4)

2-Amino-3′,6′-bis(diethylamino)spiro[isoindoline-1,9′-xanthen]-3-one (**2**) (263 mg, 0.57 mmol) prepared according to the previous report [20a] was dissolved in EtOH (6 mL). Then, 6-chloro-4-oxo-4*H*-chromene-3-carbaldehyde (**3**) [22] (132 mg, 0.63 mmol) was added. The reaction mixture was stirred and heated at reflux for 1 h, at the end of which time it was cooled and filtered. The solid was washed with EtOH and dried to afford **4** as a gray–yellow solid: 295 mg (79%); mp 258–263 °C; IR (KBr), υ: 3089, 3074, 3036, 2968, 2926, 2892, 2868, 1693, 1612, 1515, 1465, 1306, 1216, 1117, 784, 639, 471 cm^{-1}; ^{1}H NMR ($CDCl_3$, 400 MHz), δ (ppm): 1.15 (*t*, 12H, NCH_2CH_3, *J* = 7.0 Hz), 3.32 (q, 8H, NCH_2CH_3, *J* = 7.0 Hz), 6.33 (d, 2H, Xanthene—H, *J* = 7.3 Hz), 6.47 (s, 2H, Xanthene–H), 6.49 (d, 2H, Xanthene—H, *J* = 7.3 Hz), 7.11 (d, 1H, Ar—H, *J* = 6.9 Hz), 7.35 (d, 1H, Chromone—H, *J* = 8.9 Hz), 7.44–7.52 (m, 2H, Ar—H), 7.54 (dd, 1H, Chromone—H, *J* = 8.9, 2.6 Hz), 8.00 (d, 1H, Ar—H, *J* = 6.8 Hz), 8.11 (d, 1H, Chromone—H, *J* = 2.5 Hz), 8.40 (s, 1H, N=CH), 8.73 (s, 1H, Chromone—H); ^{13}C NMR ($CDCl_3$, 100 MHz), δ (ppm): 174.3, 165.0, 154.4, 153.8, 153.2, 149.0, 139.5, 133.8, 133.5, 131.4, 129.0, 128.3, 127.9, 125.4, 125.1, 123.9, 123.5, 120.1, 119.9 108.0, 105.7, 105.0, 98.2, 66.1, 44.4, 12.7; HRESIMS calcd for $[M+H]^+$ $C_{38}H_{36}ClN_4O_4^+$: 647.2420, found: 647.2404.

Results and discussion

*Synthesis and characterization of **4***

The synthetic strategy adopted for the synthesis of novel probe **4** is outlined in Scheme 1. Probe **4** was synthesized in a facile manner from rhodamine B (**1**) and 6-chloro-4-oxo-4*H*-chromene-3-carbaldehyde (**3**) by a two-step reaction. Briefly, compound **2** was first synthesized from rhodamine B and hydrazine hydrate following the literature procedure [20a]. Probe **4** was then easily synthesized by the reaction of **2** with **3** in 79% yield according to our previous report [21].

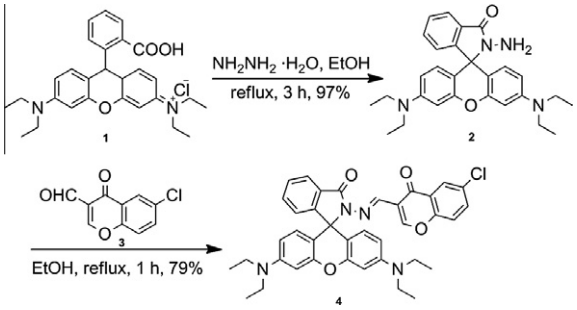

Scheme 1. Synthesis of compound **4**.

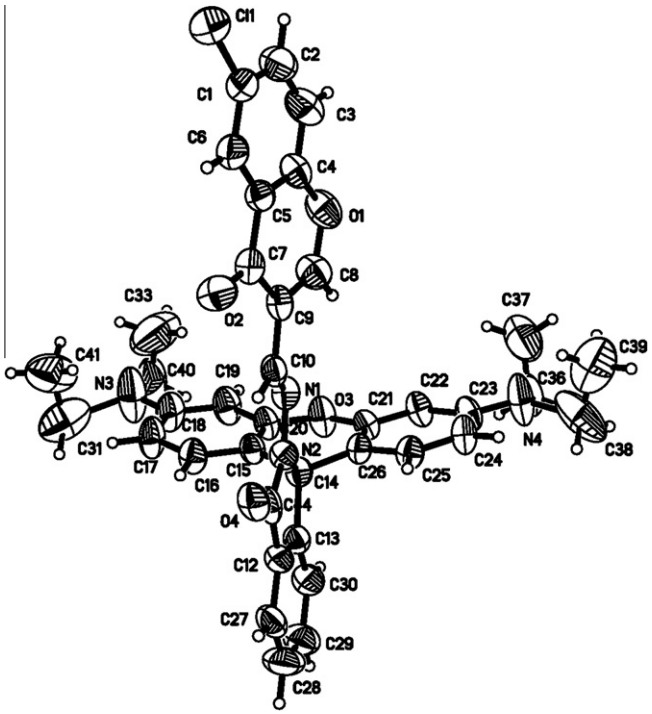

Fig. 1. The molecular structure of compound **4**.

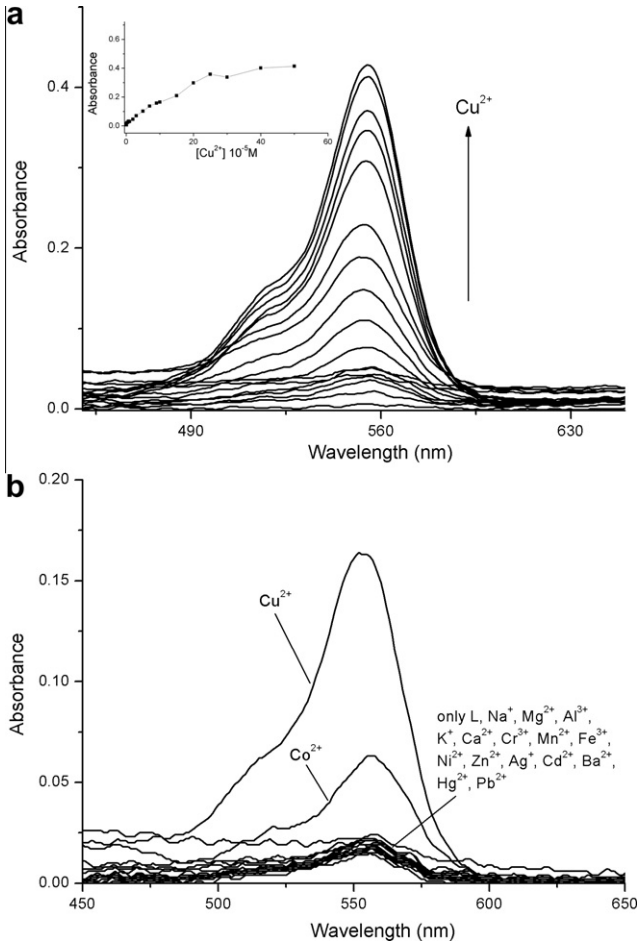

Fig. 2. (a) Absorption spectra of 10 μM **4** upon the addition of Cu^{2+} (0–50 equiv.) in CH_3CN/HEPES (20 mM, pH 7.2, 3:7, v/v) solution. The inset shows the absorbance of **4** at 553 nm as a function of Cu^{2+} concentration. (b) Absorption spectra of 10 μM **4** in buffered CH_3CN/HEPES solution with 10 equiv. of metal ions: blank, Na^+, Mg^{2+}, Al^{3+}, K^+, Ca^{2+}, Cr^{3+}, Mn^{2+}, Fe^{3+}, Co^{2+}, Ni^{2+}, Zn^{2+}, Ag^+, Cd^{2+}, Ba^{2+}, Pb^{2+}, Hg^{2+} and Cu^{2+} ions.

Structure of probe **4** was ascertained by HRMS data and ^1H NMR and ^{13}C NMR spectra. Similar to other rhodamine spirolactam derivatives, compound **4** forms a nearly colorless and fluorescence inactive solution either in buffered (20 mM HEPES, pH = 7.2) CH_3CN/HEPES (3:7, v/v) solution or pure organic solvent, indicating that the spirolactam form predominantly exists. The characteristic peak of the 9-carbon of **4** at 66.1 ppm in the ^{13}C NMR also supports this consideration [18e,23]. Moreover, a single crystal of compound **4** was obtained from CH_2Cl_2—hexane (1:1, v/v) solution and was characterized using X-ray crystallography (Fig. 1). The crystal exactly indicated the formation of a unique spirolactam-ring structure similar to our previous reported [21]. Such a special conformation of the rhodamine group makes probe **4** colorless and non-fluorescent in solution. Thus, probe **4** is expected to act as a signal switcher, which is envisioned to turn-on when the target cation is bound.

Spectral characteristics and optical responses to Cu^{2+}

As expected, probe **4** hardly reveals absorption at 450–650 nm in buffered (20 mM HEPES, pH = 7.2) CH_3CN/HEPES (3:7, v/v) solution, indicating that **4** exists in a spirocycle-closed form. The addition of Cu^{2+} to a buffered solution of **4** (10 μM) results in an obvious pink color and bright orange fluorescence as a result of the Cu^{2+} – induced ring opening of the spirolactam form, and leads to a significant enhancement of absorbance (Fig. 2a) and fluorescence emission (Fig. 3b) in the 500–650 nm range. The fluorescence quantum yield (Φ_F) of **4** with 15 equiv. of Cu^{2+} is 0.26 at an excitation wavelength of 530 nm, which is higher than that previous reported [21], where rhodamine B (Φ_F = 0.69 in ethanol) is used as a standard [24]. Fig. S1 shows a linear response range covering a concentration range of Cu^{2+} from 0.1×10^{-5} to 7.0×10^{-5} M and the correlation coefficient R = 0.9896. The linear equation is $F = 94.1[Cu^{2+}] + 135.0$. The detection limit, based on the definition by IUPAC [25] ($C_{DL} = 3S_b/m$), is 2.3×10^{-7} M.

*Selectivity of the probe **4** to Cu^{2+} and other metal ions*

The selectivity is the most important property for developing a Cu^{2+} fluorescence probe. An important feature of **4** is its high selectivity toward the Cu^{2+} over the other competitive metal ions. A purple color developed in the presence of 10 equiv. of Cu^{2+}, but no obvious color change can be found when 10 equiv. of the other sixteen metal ions was used in buffered solution of 10 μM **4** (Fig. S2, Supporting information). Figs. 2b and 3a show the absorption and fluorescence spectra of **4** with miscellaneous metal cations respectively. The addition of Cu^{2+} caused a remarkably enhanced absorbance and fluorescence at 553 nm and 579 nm,

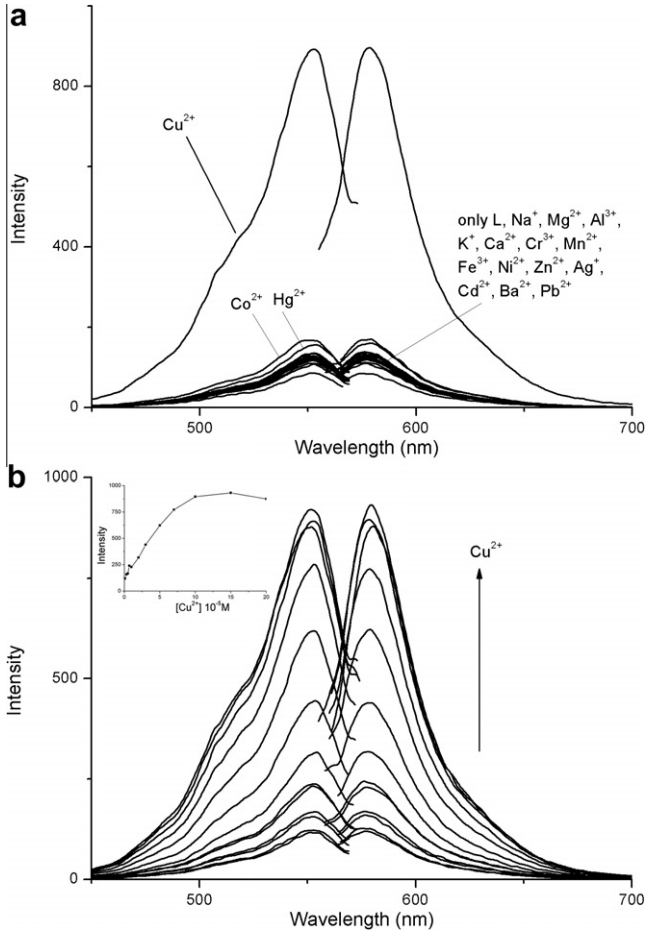

Fig. 3. (a) Fluorescence excitation and fluorescence emission spectra of 10 μM **4** in buffered CH_3CN/HEPES solution at pH 7.2 with 10 equiv. of metal ions: blank, Na^+, Mg^{2+}, Al^{3+}, K^+, Ca^{2+}, Cr^{3+}, Mn^{2+}, Fe^{3+}, Co^{2+}, Ni^{2+}, Zn^{2+}, Ag^+, Cd^{2+}, Ba^{2+}, Pb^{2+}, Hg^{2+} and Cu^{2+} ions. (b) Fluorescence excitation and fluorescence emission spectra of 10 μM **4** upon the addition of Cu^{2+} (0–20 equiv.) in buffered CH_3CN/HEPES solution. The inset shows the fluorescence intensity of **4** at 579 nm as a function of Cu^{2+} concentration. (Excitation wavelength (λ_{ex}), 553 nm; slit width, 10 nm; emission wavelength (λ_{em}), 579 nm; slit width, 2.5 nm.)

respectively. However, without cations, **4** showed weak fluorescence at 450–650 nm, and other metal ions, including Na^+, Mg^{2+}, Al^{3+}, K^+, Ca^{2+}, Cr^{3+}, Mn^{2+}, Fe^{3+}, Co^{2+}, Ni^{2+}, Hg^{2+}, Zn^{2+}, Ba^{2+}, Pb^{2+}, Ag^+ and Cd^{2+}, did not cause significant fluorescence increase also, it showed nearly no interference. The interference of coexistent metal ions and anions on the determination of Cu^{2+} was examined. Fig. 4 displays that the addition of 100 μM of other metal ions to the probe **4** with 10 μM of Cu^{2+} caused little increase of fluorescence intensity. Fig. S3 reveals that the anions caused no significant effect to the determination of Cu^{2+}. This suggests that compound **4** could serve as a highly selective "turn-on" colorimetric and fluorescent probe for Cu^{2+}.

Kinetic assay

Fig. S4 shows the time course for the fluorescence response of 10 μM **4** upon the addition of 10 equiv. Cu^{2+} in buffered solution at room temperature. The experiment suggests that the probe **4** can react with Cu^{2+} within 1–2 min, and the solution is stable to light and air. Moreover, **4**–Cu^{2+} complex was stable in buffered CH_3CN/HEPES solution for at least 2 d. These results suggest that **4** is a highly sensitive and stable fluorescence probe for Cu^{2+}.

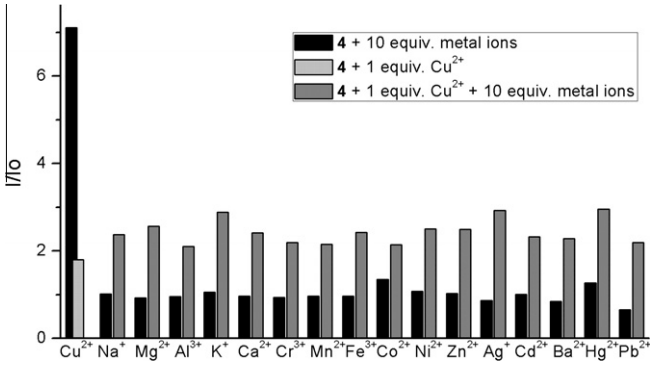

Fig. 4. Fluorescence response of 10 μM **4** to 100 μM of different metal ions (the black bar portion), 10 μM of Cu^{2+} (the light gray bar portion) and the mixture of 100 μM of other metal ions with 10 μM of Cu^{2+} (the gray bar portion). (Excitation wavelength (λ_{ex}), 553 nm; slit width, 10 nm; emission wavelength (λ_{em}), 579 nm; slit width, 2.5 nm.)

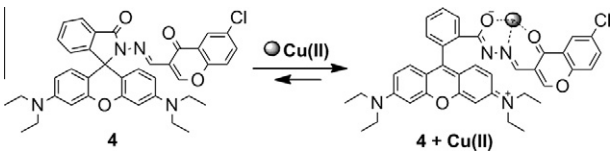

Fig. 5. The proposed binding mechanism for **4** with Cu^{2+}.

*Binding of **4** with Cu^{2+}*

In order to further investigate the binding mode of **4** and Cu^{2+}, an absorption spectra titration and Job's method were carried out. Fig. 2a showed the absorption spectra variation of **4** on the gradual addition of Cu^{2+}. Upon the gradual addition of Cu^{2+} up to 1.0 equiv. into 10 μM of **4** in buffered CH_3CN/HEPES solution, the absorbance of absorption band that peaked at 553 nm increased linearly at first and then reached its maximum when the amount of added Cu^{2+} was above 1.0 equiv. The linear fit of the data revealed that the binding of **4** to Cu^{2+} was most probably in 1:1 stoichiometry of which there was a good linear correlation ($R = 0.9942$) with an association constant (Ka) of about $0.6 \times 10^4\ M^{-1}$ which corresponds to a close binding capability toward Cu^{2+} in comparison with a rhodamine 6G derivative binding to Cu^{2+} (with a Ka value of $2.08 \times 10^4\ M^{-1}$) [18e]. The data from Job's method exhibited a maximum absorbance when the molecular fraction of **4** was close to 50%, which also suggested a 1:1 stoichiometry for **4**-Cu^{2+} complex and the extinction coefficient of **4**-Cu^{2+} complex (1:1 stoichiometry) at 553 nm is 6610 L mol^{-1} cm^{-1} which is larger than that previous reported (4570 L mol^{-1} cm^{-1}) [21], (Figs. S5 and S6, Supporting information). The HRESIMS data (calcd for $[M + Cu + H]^{3+}$ $C_{38}H_{36}ClCuN_4O_4^{3+}$: 710.1721, found: 710.2347) also established the above conclusion. The proposed binding mode is shown in Fig. 5.

Effect of pH

In order to assess the potential for live cell image applications of the probe, the effect of pH on the fluorescence of the probe was evaluated. The relative fluorescence intensity is not strongly dependent on pH between 6.7 and 7.6, close to physiological conditions (Fig. S7, Supporting information).

Fluorescence imaging of intercellular Cu^{2+}

We then examined the potential utility of the novel rhodamine chromene-based probe **4** as a Cu^{2+} probe in living cells. Incubation

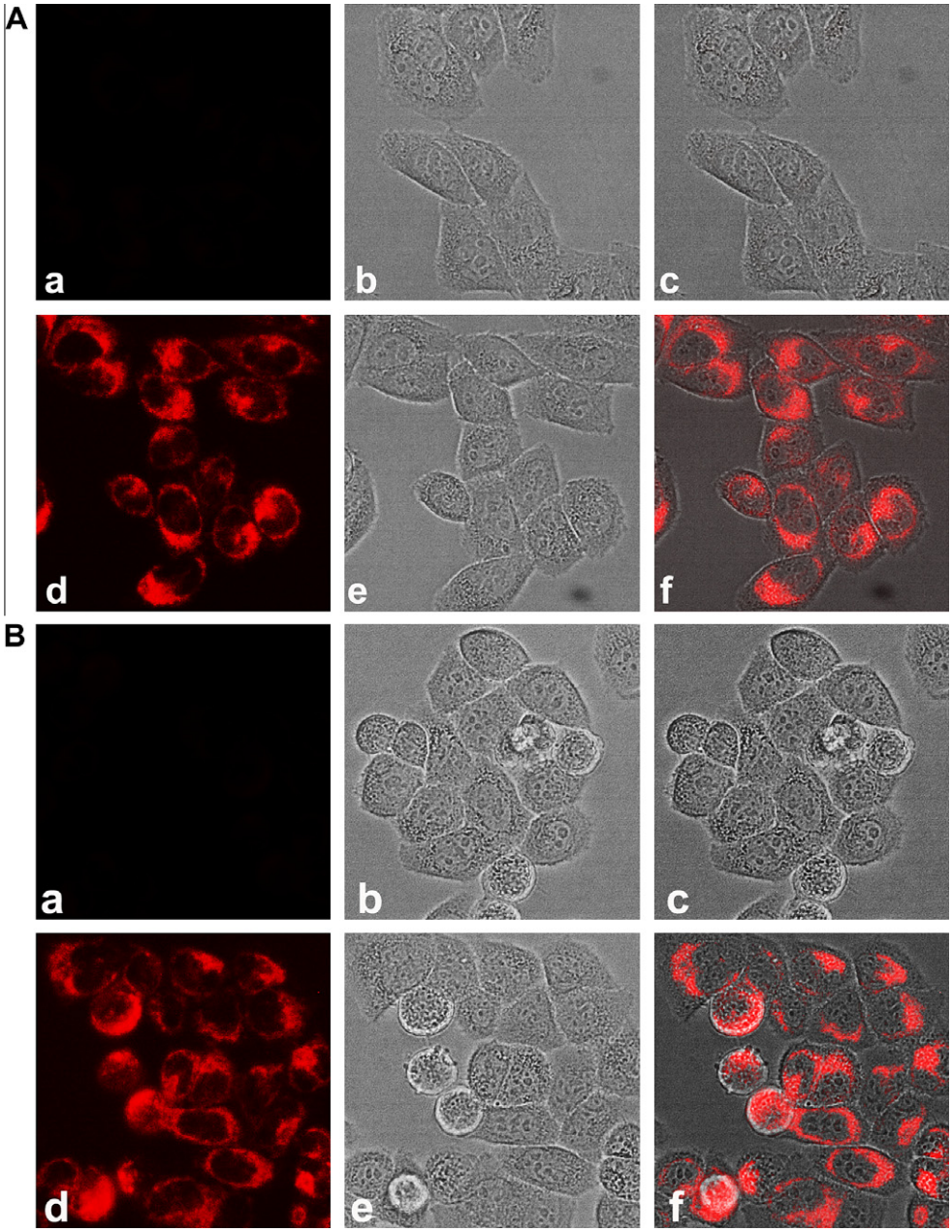

Fig. 6. Fluorescence microscope images of living HeLa cells. **A**: using $CuCl_2$; **B**: using $Cu(NO_3)_2$. (a) Cells incubated with 10 μM probe **4** for 1 h at 37 °C; (b) Bright-field view of panel (a); (c) overlay image of (a) and (b). (d) Cells with 50 μM Cu^{2+} added to the growth medium for 2 h at 37 °C and then incubated with a 10 μM probe **4** for 1 h at 37 °C. (e) Bright-field image of the live HeLa cells shown in panel (d). (f) Overlay image of (d) and (e).

of HeLa cells with 10 μM of **4** for 1 h at 37 °C gave almost no intracellular fluorescence as monitored by fluorescence microscopy (Fig. 6a). This was consistent with the previous findings that cancer cells in cell culture contain little Cu^{2+} [26]. When Hela cells were incubated with growth medium containing 50 μM of Cu^{2+} for 2 h, the same treatment with **4** generated remarkable intracellular fluorescence (Fig. 6d). Bright-field measurements after treatment with Cu^{2+} and **4** confirmed that the cells were viable throughout the imaging experiments (Fig. 6b and e). The predicted lipophilicity of **4** is stronger than that of methoxyl substituted probe in our previous work [21] (CLogP of **4**: 8.313, CLogP of methoxyl substituted probe: 7.706), and this is identical with the results of the assay. The overlay of fluorescence and images revealed that the fluorescence signals were localized in the perinuclear region of the cytosol (Fig. 6f), indicating the subcellular distribution of Cu^{2+} internalized into the living cells from the growth medium. In addition, from Fig. 6A and B we can find that in the case of $CuCl_2$ and $Cu(NO_3)_2$ images are similar. The results show that this probe can monitor intracellular Cu^{2+} in HeLa cells in shorter time.

Conclusion

In summary, we have developed a novel rhodamine chromene-based turn-on fluorescence probe to monitor intracellular Cu^{2+} level in living cells. The probe switches to a highly fluorescent complex upon Cu^{2+} chelation under physiological conditions. The high sensitivity and selectivity of the probe are demonstrated by a remarkable fluorescence enhancement and the lack of interference from up to 16 other metal ions. Furthermore, this probe that possesses chlorine group instead of methoxyl group has more lipophilicity and can monitor intracellular Cu^{2+} in HeLa cells in shorter time.

Acknowledgments

This study was supported by 973 Program (2010CB933504) and the National Natural Science Foundation of China (20972088 and 90813022).

Appendix A. Supplementary material

Electronic Supplementary Information (ESI) available: Supplementary figures S1–S11. CCDC reference number 825977 contains the supplementary crystallographic data for this paper. These data can be obtained free of charge via www.ccdc.cam.ac.uk/data_request/cif, by emailing data_request@ccdc.cam.ac.uk, or by contacting The Cambridge Crystallographic Data Centre, 12, Union Road, Cambridge CB21EZ, UK; fax: +44 1223 336033. Supplementary data associated with this article can be found, in the online version, at http://dx.doi.org/10.1016/j.saa.2012.04.073.

References

[1] D.G. Barceloux, J. Toxicol. Clin. Toxicol. 37 (1999) 217–230.
[2] (a) P.C. Bull, G.R. Thomas, J.M. Rommens, J.R. Forbes, D.W. Cox, Nat. Genet. 5 (1993) 327–337;
(b) J.S. Valentine, P.J. Hart, Proc. Natl. Acad. Sci. USA 100 (2003) 3617–3622;
(c) Y.H. Hung, A.I. Bush, R.A. Cherny, J. Biol. Inorg. Chem. 15 (2010) 61–76;
(d) M. Taki, S. Iyoshi, A. Ojida, I. Hamachi, Y. Yamamoto, J. Am. Chem. Soc. 132 (2010) 5938–5939.
[3] V.L. Goodman, G.J. Brewer, S.D. Merajver, Endocr. Relat. Cancer 11 (2004) 255–263.
[4] (a) G. Muthaup, A. Schlicksupp, L. Hess, D. Beher, T. Ruppert, C.L. Masters, K. Beyreuther, Science 271 (1996) 1406–1409;
(b) R.A. Løvstad, BioMetals 17 (2004) 111–113.
[5] (a) S. Goswami, D. Sen, N.K. Das, G. Hazra, Tetrahedron Lett. 51 (2010) 5563–5566;
(b) D.Y. Lee, N. Singh, M.J. Kim, D.O. Jang, Tetrahedron 66 (2010) 7965–7969;
(c) M. Alfonso, A. Tárraga, P. Molina, Dalton Trans. 39 (2010) 8637–8645;
(d) C.I.C. Esteves, M.M.M. Raposo, S.P.G. Costa, Tetrahedron 66 (2010) 7479–7486;
(e) Z. Su, K.Y. Chen, Y. Guo, H.P. Qi, X.F. Yang, M.L. Zhao, J. Fluoresc. 20 (2010) 851–856;
(f) X.B. Huang, J. Meng, Y. Dong, Y.X. Cheng, C.J. Zhu, Polymer 51 (2010) 3064–3067;
(g) A.R. Bayles, H.S. Chahal, D.S. Chahal, C.P. Goldbeck, B.E. Cohen, B.A. Helms, Nano Lett. 10 (2010) 4086–4092;
(h) C. Petibois, Anal. Bioanal. Chem. 397 (2010) 2051–2065;
(i) Y.M. Wang, M.X. Yu, Y.H. Yu, Z.P. Bai, Z. Shen, F.Y. Li, X.Z. You, Tetrahedron Lett. 50 (2009) 6169–6172;
(j) M.Y. Yu, M. Shi, Z.G. Chen, F.Y. Li, X.X. Li, Y.H. Gao, J. Xu, H. Yang, Z.G. Zhou, T. Yi, C.H. Huang, Chem. Eur. J. 14 (2008) 6892–6900;
(k) P.X. Xi, J.Y. Dou, L. Huang, M. Xu, F.J. Chen, Y.J. Wu, D.C. Bai, W.G. Li, Z.Z. Zeng, Sens. Actuators B: Chem. 148 (2010) 337–341.
[6] (a) L. Huang, J. Cheng, K. Xie, P. Xi, F. Hou, Z. Li, G. Xie, Y. Shi, H. Liu, D. Bai, Z. Zeng, Dalton Trans. 40 (2011) 10815–10817;
(b) Z. Zhou, N. Li, A. Tong, Anal. Chim. Acta 702 (2011) 81–86;
(c) K.C. Ko, J.S. Wu, H.J. Kim, P.S. Kwon, J.W. Kim, R.A. Bartsch, J.Y. Lee, J.S. Kim, Chem. Commun. 47 (2011) 3165–3167.
[7] S. Sirilaksanapong, M. Sukwattanasinittb, P. Rashatasakhon, Chem. Commun. 48 (2012) 293–295.
[8] J. Jiang, H. Jiang, X. Tang, L. Yang, W. Dou, W. Liu, R. Fang, W. Liu, Dalton Trans. 40 (2011) 6367–6370.
[9] K. Kaur, S. Kumar, Dalton Trans. 40 (2011) 2451–2458.
[10] (a) D. Liu, Z. Wang, X. Jiang, Nanoscale 3 (2011) 1421–1433;
(b) Y.W. Lin, C.C. Huang, H.T. Chang, Analyst 136 (2011) 863–871.
[11] H.N. Kim, Z. Guo, W. Zhu, J. Yoon, H. Tian, Chem. Soc. Rev. 40 (2011) 79–93.
[12] J.R. Lakowicz, Principles of Fluorescence Spectroscopy, third ed., Springer, New York, 2006. pp. 67.
[13] M.E. Jun, K.H. Ahn, Org. Lett. 12 (2010) 2790–2793.
[14] (a) Z.X. Han, X.B. Zhang, Z. Li, Y.J. Gong, X.Y. Wu, Z. Jin, C.M. He, L.X. Jian, J. Zhang, J.L. Shen, R.Q. Yu, Anal. Chem. 82 (2010) 3108–3113;
(b) S.H. Mashraqui, T. Khan, S. Sundaram, R. Betkar, M. Chandiramani, Chem. Lett. 38 (2009) 730–731.
[15] (a) J. Mao, Q. He, W.S. Liu, Talanta 80 (2010) 2093–2098;
(b) Y. Xiang, Z. Li, A. Tong, Luminescence 23 (2008) 103;
(c) S. Wang, X. Meng, M. Zhu, Tetrahedron Lett. 52 (2011) 2840–2843.
[16] (a) Y. Wan, Q.J. Guo, X.F. Wang, A.D. Xia, Anal. Chim. Acta 665 (2010) 215–220;
(b) K.W. Huang, H. Yang, Z.G. Zhou, M.X. Yu, F.Y. Li, X. Gao, T. Yi, C.H. Huang, Org. Lett. 10 (2008) 2557–2560.
[17] (a) J.J. Du, J.L. Fan, X.J. Peng, P.P. Sun, J.Y. Wang, H.L. Li, S.G. Sun, Org. Lett. 12 (2010) 476–479;
(b) Y. Zhao, Y. Sun, X. Lv, Y.L. Liu, M.L. Chen, W. Guo, Org. Biomol. Chem. 8 (2010) 4143–4147;
(c) W.Y. Lin, X.W. Cao, Y.D. Ding, L. Yuan, Q.X. Yu, Org. Biomol. Chem. 8 (2010) 3618–3620;
(d) X.L. Zhang, Y. Xiao, X.H. Qian, Angew. Chem. Int. Ed. 47 (2008) 8025–8029;
(e) Q.J. Ma, X.B. Zhang, X.H. Zhao, Z. Jin, G.J. Mao, G.L. Shen, R.Q. Yu, Anal. Chim. Acta 663 (2010) 85–90;
(f) H. Wang, Y. Li, S. Xu, Y. Li, C. Zhou, X. Fei, L. Sun, C. Zhang, Y. Li, Q. Yang, X. Xu, Org. Biomol. Chem. 9 (2011) 2850–2855.
[18] (a) M. Dong, T.H. Ma, A.J. Zhang, Y.M. Dong, Y.W. Wang, Y. Peng, Dyes Pigm. 87 (2010) 164–172;
(b) L. Huang, X. Wang, G.Q. Xie, P.X. Xi, Z.P. Li, M. Xu, Y.J. Wu, D.C. Bai, Z.Z. Zeng, Dalton Trans. 39 (2010) 7894–7896;
(c) G.H. Wu, D.X. Wang, D.Y. Wu, Y. Gao, Z.Q. Wang, J. Chem. Sci. 121 (2009) 543–548;
(d) F.B. Yu, W.S. Zhang, P. Li, Y.L. Xing, L.L. Tong, J.P. Ma, B. Tang, Analyst 134 (2009) 1826–1833;
(e) Y. Zhao, X.B. Zhang, Z.X. Han, L. Qiao, C.Y. Li, L.X. Jian, G.L. Shen, R.Q. Yu, Anal. Chem. 81 (2009) 7022–7030;
(f) X. Zhang, S. Sumiya, Y. Shiraishi, T. Hirai, J. Photochem. Photobiol. A Chem. 205 (2009) 215–220;
(g) Y. Zhou, F. Wang, Y. Kim, S.J. Kim, J. Yoon, Org. Lett. 11 (2009) 4442–4445;
(h) X.Q. Chen, J. Jia, H.M. Ma, S.J. Wang, X.C. Wang, Anal. Chim. Acta 632 (2009) 9–14;
(i) Z.H. Xu, L.K. Zhang, R. Guo, T.C. Xiang, C.Z. Wu, Z. Zheng, F.L. Yang, Sens. Actuators B: Chem. 156 (2011) 546–552.
[19] (a) K.R. Surati, B.T. Thaker, J. Coord. Chem. 59 (2006) 1191–1202;
(b) K.M. Vyas, R.N. Jadeja, V.K. Gupta, K.R. Surati, J. Mol. Struct. 990 (2011) 110–120.
[20] (a) Y. Xiang, A.J. Tong, P.Y. Jin, Y. Ju, Org. Lett. 8 (2006) 2863–2866;
(b) K.M.K. Swamy, S.K. Ko, S.K. Kwon, H.N. Lee, C. Mao, J.M. Kim, K.H. Lee, J. Kim, I. Shin, J. Yoon, Chem. Commun. 45 (2008) 5915–5917;
(c) C.W. Yu, J. Zhang, R. Wang, L.X. Chen, Org. Biomol. Chem. 8 (2010) 5277–5279;
(d) X. Zeng, L. Dong, C. Wu, L. Mu, S.F. Xue, Z. Tao, Sens. Actuators B Chem. B141 (2009) 506–510;
(e) X.Q. Chen, M.J. Jou, H. Lee, S. Kou, J. Lim, S.W. Nam, S. Park, K.M. Kim, J. Yoon, Sens. Actuators B Chem. B137 (2009) 597–602;
(f) J. Zhang, C.W. Yu, S.Y. Qian, G. Lu, J.L. Chen, Dyes Pigm. 92 (2012) 1370–1375;
(g) H.N. Kim, S.W. Nam, K.M.K. Swamy, Y. Jin, X.Q. Chen, Y. Kim, S.J. Kim, S. Park, J. Yoon, Analyst 136 (2011) 1339–1343;
(h) H. Yang, Z.G. Zhou, K.W. Huang, M.X. Yu, F.Y. Li, T. Yi, C.H. Huang, Org. Lett. 9 (2007) 4729–4732;
(i) L. Jiang, L. Wang, B. Zhang, G. Yin, R.Y. Wang, Eur. J. Inorg. Chem. 28 (2010) 4438–4443;
(j) L.J. Tang, F.F. Li, M.H. Liu, R. Nandhakumar, Spectrochim. Acta A Mol. Biomol. Spectrosc. 78A (2011) 1168–1172.
[21] W.Y. Liu, H.Y. Li, B.X. Zhao, J.Y. Miao, Org. Biomol. Chem. 9 (2011) 4802–4805.
[22] T. Patonay, A. Kiss-Szikszai, V.M.L. Silva, A.M.S. Silva, D.C.G.A. Pinto, J.A.S. Cavaleiro, J. Jekö, Eur. J. Org. Chem. 2008 (2008) 1937–1946.
[23] U. Anthoni, C. Christophersen, P. Nielsen, A. Puschl, K. Schaumburg, Struct. Chem. 6 (1995) 161–165.
[24] C.A. Parker, W.T. Rees, Analyst 85 (1960) 587–600.
[25] H.M.N.H. Irving, H. Freiser, T.S. West (Eds.), IUPAC Compendium of Analytical Nomenclature, Definitive Rules, Pergamon Press, Oxford, 1981.
[26] K.G. Daniel, P. Gupta, R.H. Harbach, W.C. Guida, Q.P. Dou, Biochem. Pharmacol. 67 (2004) 1139–1151.